

UCSF

UC San Francisco Previously Published Works

Title

Lucanthone and Its Derivative Hycanthone Inhibit Apurinic Endonuclease-1 (APE1) by Direct Protein Binding

Permalink

<https://escholarship.org/uc/item/57r3s0g3>

Journal

PLOS ONE, 6(9)

ISSN

1932-6203

Authors

Naidu, Mamta D
Agarwal, Rakhi
Pena, Louis A
et al.

Publication Date

2011

DOI

10.1371/journal.pone.0023679

Peer reviewed

Lucanthone and Its Derivative Hycanthone Inhibit Apurinic Endonuclease-1 (APE1) by Direct Protein Binding

Mamta D. Naidu^{1*}, Rakhi Agarwal¹, Louis A. Pena², Luis Cunha³, Mihaly Mezei⁴, Min Shen⁵, David M. Wilson, III⁶, Yuan Liu⁷, Zina Sanchez⁸, Pankaj Chaudhary¹, Samuel H. Wilson⁷, Michael J. Waring⁹

1 Biology Department, Brookhaven National Laboratory, Upton, New York, United States of America, **2** Medical Department, Brookhaven National Laboratory, Upton, New York, United States of America, **3** Department of Genetics and Genomic Sciences, Mount Sinai School of Medicine, New York, New York, United States of America, **4** Department of Structural and Chemical Biology, Mount Sinai School of Medicine, New York, New York, United States of America, **5** NIH Chemical Genomics Center, National Institutes of Health, Rockville, Maryland, United States of America, **6** Laboratory of Molecular Gerontology, Biomedical Research Center, National Institute on Aging, National Institutes of Health (NIH), Baltimore, Maryland, United States of America, **7** Laboratory of Structural Biology, National Institute of Environmental Health Sciences, National Institutes of Health (NIH), Research Triangle Park, North Carolina, United States of America, **8** Undergraduate Biology, Stony Brook University, Stony Brook, New York, United States of America, **9** Department of Pharmacology, University of Cambridge, Cambridge, United Kingdom

Abstract

Lucanthone and hycanthone are thioxanthenone DNA intercalators used in the 1980s as antitumor agents. Lucanthone is in Phase I clinical trial, whereas hycanthone was pulled out of Phase II trials. Their potential mechanism of action includes DNA intercalation, inhibition of nucleic acid biosyntheses, and inhibition of enzymes like topoisomerases and the dual function base excision repair enzyme apurinic endonuclease 1 (APE1). Lucanthone inhibits the endonuclease activity of APE1, without affecting its redox activity. Our goal was to decipher the precise mechanism of APE1 inhibition as a prerequisite towards development of improved therapeutics that can counteract higher APE1 activity often seen in tumors. The IC₅₀ values for inhibition of APE1 incision of depurinated plasmid DNA by lucanthone and hycanthone were 5 μM and 80 nM, respectively. The K_D values (affinity constants) for APE1, as determined by BIACORE binding studies, were 89 nM for lucanthone/10 nM for hycanthone. APE1 structures reveal a hydrophobic pocket where hydrophobic small molecules like thioxanthenones can bind, and our modeling studies confirmed such docking. Circular dichroism spectra uncovered change in the helical structure of APE1 in the presence of lucanthone/hycanthone, and notably, this effect was decreased (Phe266Ala or Phe266Cys or Trp280Leu) or abolished (Phe266Ala/Trp280Ala) when hydrophobic site mutants were employed. Reduced inhibition by lucanthone of the diminished endonuclease activity of hydrophobic mutant proteins (as compared to wild type APE1) supports that binding of lucanthone to the hydrophobic pocket dictates APE1 inhibition. The DNA binding capacity of APE1 was marginally inhibited by lucanthone, and not at all by hycanthone, supporting our hypothesis that thioxanthenones inhibit APE1, predominantly, by direct interaction. Finally, lucanthone-induced degradation was drastically reduced in the presence of short and long lived free radical scavengers, e.g., TRIS and DMSO, suggesting that the mechanism of APE1 breakdown may involve free radical-induced peptide bond cleavage.

Citation: Naidu MD, Agarwal R, Pena LA, Cunha L, Mezei M, et al. (2011) Lucanthone and Its Derivative Hycanthone Inhibit Apurinic Endonuclease-1 (APE1) by Direct Protein Binding. PLoS ONE 6(9): e23679. doi:10.1371/journal.pone.0023679

Editor: Fernando Rodrigues-Lima, University Paris Diderot-Paris 7, France

Received: September 24, 2010; **Accepted:** July 23, 2011; **Published:** September 15, 2011

This is an open-access article, free of all copyright, and may be freely reproduced, distributed, transmitted, modified, built upon, or otherwise used by anyone for any lawful purpose. The work is made available under the Creative Commons CC0 public domain dedication.

Funding: This work was supported by DOE grant KP-1401020/MO-079, NIH grant R01-CA86897, the Intramural Research Program of the National Institute on Aging and the Intramural Research Program of the NIH, National Institutes of Environmental Health Sciences (Z01ES050158 & Z01-ES050159). The funders had no role in study design, data collection and analysis, decision to publish, or preparation of the manuscript.

Competing Interests: The authors have declared that no competing interests exist.

* E-mail: mnaidu@bnl.gov

Introduction

APE1 (also termed Ref-1, APEX, HAP1, AP endo) is a multifunctional protein with distinct activities assigned to different parts of its structure. The N-terminal region is responsible for its redox function, whereas the endonuclease activity is mediated by the larger C-terminal portion [1–3]. APE1 is abundant in human cells and accounts for nearly all of the apurinic/aprimidinic (AP) site cleavage activity found in cellular extracts [4]. APE1 has a strong Mg²⁺-dependent AP endonuclease activity, a 3'-phosphodiesterase activity, a 3'-mismatch exonuclease activity, and in addition to its DNA repair functions, a redox activity whereby it can reduce a conserved cysteine residue in a target transcription factor,

e.g. AP-1 (Jun/Fos), to activate cognate DNA binding. APE1 also stimulates the sequence-specific DNA binding activities of HIFα, NFκB, Pax5, Pax8, Myb and related activating transcription factor/cAMP-responsive element binding proteins [5].

APE1 incision activity is altered in response to radiation and chemotherapy in medulloblastoma and primitive neuroectodermal tumors [6]. Silber *et al.* also showed that APE1 repair activity, which is increased by oxidative stress, contributes to resistance of human glioma cells to alkylating agents [7]. Human glioma cell lines that show lower APE1 expression were more sensitive to methyl methanesulfonate (MMS) and H₂O₂, known inducers of AP sites and single strand breaks in DNA [8]. Robertson *et al.* [9] have shown that over-expression of APE1 in NT2 cells confers

resistance to bleomycin and radiation. Recently, we demonstrated a correlation between APE1 and radiation sensitivity with glioma cell culture models [10]. When APE1 was over-expressed in U251 cells, they became more radioresistant contingent on the level of APE1 over-expression, whereas siRNA depletion of APE1 was associated with radiation sensitivity. This correlation was reiterated by recent studies where APE1 siRNA down-regulation in either colorectal tumor cells *in vitro* or in a subcutaneous nude mouse colon cancer model enhanced radiosensitivity as revealed by increased apoptosis [11]. In addition to the siRNA studies, we modulated APE1 repair nuclease function using two of its known small molecule inhibitors, lucanthone (1-[2-diethylaminoethylamino]-4-methylthioxanthen-9-one) [12] and CRT0044876 (7-Nitroindole-2-carboxylic acid) [13], and showed that APE1 inhibition resulted in increased radiosensitivity.

Due to the dual function of APE1, several inhibitors are being discovered which selectively inhibit either its DNA repair or redox function. The DNA repair inhibitors include the indirect inhibitor methoxamine (MX) [5,14] and the direct/indirect inhibitors such as lucanthone and CRT0044876. The redox function (Ref-1) inhibitors are soy isoflavones [15], E3330 [16–17] and its benzquinone and naphthoquinone analogues [18], PRNI-299 [19], BQP [20] and resveratrol [21]. Thus, recent efforts have focused on the potential to strategically regulate APE1 protein activity in cells, possibly through the use of small molecular inhibitors, as a means of improving therapeutic agent response.

Lucanthone (CAS479-50-5) and hycanthone (CAS3105-97-3) belong to a family of thioxanthenones and were originally synthesized for use as anti-schistosomal drugs. They were also determined to be DNA intercalators, and like actinomycin D, inhibited RNA synthesis as well as the DNA processing enzymes topoisomerases I and II [22]. The effects of lucanthone are thought to be mediated by its bioactive metabolite, hycanthone [23]. Hycanthone was shown to be a better anti-schistosomal [24] agent than lucanthone. However, due to the negative side effects of hycanthone, including acute hepatic necrosis [25], strong mutagenicity [26] and weak carcinogenicity [27], the use of hycanthone for treatment of human schistosomiasis has been discontinued. Lucanthone, on the other hand, has been used to treat schistosomiasis for almost 20 years before being replaced by new drugs. Work by Turner *et al* [28] showed that radiolabeled lucanthone was more concentrated in neoplastic tissue relative to the surrounding muscle and skin. Since lucanthone is able to cross the blood brain barrier and inhibit cell proliferation without affecting normal non-cycling cells, the compound has been used as an adjuvant for brain tumor radiotherapy [29] and is currently in clinical trial.

Lucanthone is known to inhibit APE1 AP endonuclease activity, without affecting its redox function [12]. Lucanthone is also known to promote accumulation of AP sites in HeLa cells [30], lesions that are substrates for APE1. Since Bailly *et al* [31] showed that both lucanthone and hycanthone preferentially intercalate at AT-rich sequences in DNA, APE1 may be prevented from accessing the AP site due to the presence of DNA-bound lucanthone/hycanthone. Alternatively, lucanthone may elicit its inhibitory effect on APE1 incision activity via direct binding to the protein. As previously reported APE1 structures (PDB ID: 2ISI, 1DEW and 1DE9) show the presence of a hydrophobic site lined by Phe266, Trp280 and Leu282, overlapping the active site of the protein, we hypothesized that hydrophobic molecules like lucanthone/hycanthone would bind at these residues. In addition, based on past evidence [32], we postulated that lucanthone/hycanthone may induce protein oxidation due to the binding capacity and other features of the compound. Data are presented

here in support of the idea that lucanthone and its structural analogue hycanthone show very little, if any, inhibition of the DNA (depurinated) binding capacity of APE1 and can indeed predominantly inhibit APE1 endonuclease activity by direct binding to the hydrophobic site and inducing cleavage of the protein via oxidative damage.

Materials and Methods

Reagents

The U251-MG glioblastoma multiforme (GBM) cell line was a kind gift from Dr. Dennis Deen of UCSF. These cells were maintained in Eagle's Minimal Essential Medium with 2 mM L-glutamine and 1.5 g/L sodium bicarbonate, supplemented with 10% fetal bovine serum (FBS), and sub-cultured twice a week (1:3). Cell culture media and FBS were obtained from Invitrogen (Carlsbad, CA). APE1 protein was detected using polyclonal anti-APE1 (Santa Cruz Biotechnology, Santa Cruz, CA) and tubulin was detected using polyclonal anti- α -tubulin (Sigma-Aldrich, St. Louis, MO). ECL kit from Invitrogen has anti-mouse and anti-rabbit -HRP conjugated secondary antibodies which were used at 1: 30,000 dilution. Lucanthone and hycanthone (Figure S1) obtained (in 1970s by Michael Waring) from Dr S. Archer, Sterling-Winthrop Research Institute, Rensselaer, NY, were maintained at 4C under hygroscopic conditions, and were dissolved in sterile double distilled water just prior to reactions. Plasmids consisting of full length APE-1 in pET15b and pCMV10 were kind gifts from Dr. T. Izumi and Dr. Hua Fung, of Louisiana State Health Center, New Orleans, LA and Harvard Medical School, Boston, respectively.

Cells extract preparation

$0.5-1.5 \times 10^6$ cells were resuspended in 200 μ l of ice-cold $1 \times$ cell extraction buffer (50 mM Tris-HCl pH 7.5, 1 mM EDTA, 100 mM NaCl and 1 mM PMSF) and sonicated for 5–10 s in a 4°C bath sonicator (Sonifier Cell Disruptor, Plainview, NY) at a setting of 20 MHz. The sonicates were centrifuged at 10,000 rpm for 5 min at 4°C. Soluble and insoluble fractions were collected (the insoluble pellet was resuspended in 200 μ l of cell extraction buffer) and assayed for APE1 protein and enzyme activity as described below.

Expression and purification of full length APE1

E.coli BL21/DE3 were transformed with the pET15b plasmid containing full length APE1 and these bacterial cultures (500 ml YTB medium) were grown to OD₆₀₀ of 0.6 and the full length APE1 protein was successfully expressed and purified to 25–30 mg protein/L (20 mM HEPES, 200 mM NaCl buffer pH 7.5) culture according to method of Agarwal *et al* [33]. Additional stocks of wild-type, full length APE1, and the APE1 mutant proteins (e.g. F266A), were generated as described [34]. A pCMV-APE1 plasmid [19] was transfected into U251 cells using Lipofectamine 2000 as per manufacturer's instructions followed by selection in G418 as detailed in our recent paper [10] and clones selected for APE1 overexpression.

SDS-PAGE and Western blot

Total purified protein concentration was determined by the ratio of A₂₈₀/A₂₆₀. 250 ng of APE1 treated with lucanthone or hycanthone (0.05–100 μ M) for 2 h at 37°C in final volume of 30 μ l were mixed with an equal volume of gel loading buffer (0.001% bromophenol blue, 4% SDS, 10% 2-ME, 20% glycerol, and 125 mM Tris pH 6.8) and denatured at 95°C for 5 min. Total protein concentration in cell extracts was determined using

the Bradford assay (BioRad, Hercules, CA) and 25 μg of total protein from soluble or insoluble cell fractions were mixed with an equal volume of gel loading buffer (0.001% bromophenol blue, 4% SDS, 10% 2-ME, 20% glycerol, and 125 mM Tris pH 6.8) and denatured at 95°C for 5 min. This mixture was separated by SDS-PAGE (4% stacking, 7.5% resolving gel) for 2–3 h at 40 mA on a BioRad MiniPROTEAN II Electrophoresis Cell. To detect proteins, proteins were transferred onto a trans-Blot nitrocellulose membrane (0.45 μm ; BioRad) overnight at 4°C at 15 mA in standard Tris-Glycine buffer containing 20% ethanol. Membranes were probed using polyclonal anti-APE1 or polyclonal anti- α -tubulin at 1/1,000 dilution in TTBS (0.1% Tween 20 in TBS (pH 7.5)) with secondary, anti-rabbit HRP-conjugated antibody used at 1/30,000 dilution to detect APE1 and α -tubulin protein control. Chemi-luminescence was developed using an ECL kit according to the manufacturer's instructions and detected by exposing the blot to HyperfilmECL for 30 s–3 min. (GE Healthcare Biosciences, Piscataway, NJ).

APE1 Endonuclease activity

APE1 endonuclease activity was determined using an assay that measures the conversion of plasmid DNA from supercoiled to relaxed form by incision at an abasic site [35–36]. Briefly, the substrate used was 200 ng of dephosphorylated pUC18 DNA in 10 μl of 1 \times APE1 buffer containing 50 mM Hepes, pH 7.4, 150 mM KCl, 5 mM MgCl_2 and 100 $\mu\text{g}/\text{ml}$ of BSA in presence of different concentrations of the cell extract (1 μl containing 0–55 ng of total protein). Similar reactions mixtures were set up with untreated pUC18, which served as the internal control. This reaction mixture was incubated at 37°C for 15 min, and the reaction was stopped by addition of alkaline stop mix (0.25% bromocresol green in 0.25N NaOH, 50% glycerol) and left at room temperature for 10–15 min. Then the products were resolved on a 0.8% agarose gel in 40 mM Tris-acetate and 2 mM EDTA for 2 h. The gel was stained with ethidium bromide to visualize supercoiled and relaxed plasmid DNA and imaged with a digital imaging system [37] and the area under the supercoiled and relaxed form was determined. Final calculations were done in femtomoles (fmol) of abasic sites incised/min/mg protein with normalization done using Pyruvate Kinase units (PKU) present in these extracts. Poisson distribution calculations were done on supercoiled and relaxed bands to estimate incisions per plasmid molecule and the resulting dephosphorylated pUC18 had 1 AP site per molecule. The endonuclease activity inhibition by lucanthone was analyzed using standard Lineweaver-Burke Plot to determine if the inhibition was competitive or non-competitive.

Cleavage of APE1 by lucanthone and CRT0044876

Western blotting was carried out by 7.5% SDS-PAGE of cell extracts (20 μg total protein per lane) either from APE1 overexpresser clone 5 pretreated with 2.5–200 μM concentration of lucanthone/CRT0044876 or recombinant APE1 for 2 h at 37°C in presence of protease inhibitor cocktail (2 tablets (Roche, # 11836153001) containing mixture of several protease inhibitors with broad inhibitory specificity for serine, cysteine and metallo-proteases in all systems, dissolved in 20 ml of APE1 buffer). CRT0044876 was used as another APE1 small molecule inhibitor with possible direct interaction between itself and APE1 [13]. Pretreatment of Ape1 overexpresser clone 5 cultures with 10 $\mu\text{g}/\text{ml}$ of cycloheximide (CHX) for 4 h prior to lucanthone/hycanthone addition, was carried out to determine if these thioxanthenones affected Ape1 protein synthesis. Radioquenchers like 10 mM TRIS, ascorbic acid (100 μM), N-acetyl cysteine

(100 μM) (with recombinant APE1) or 1% DMSO (with cell extracts) were used to inhibit the cleavage reactions.

Direct binding of APE1 to lucanthone/hycanthone

APE1 (and its hydrophobic mutants) and lucanthone/hycanthone reaction stoichiometry was studied using surface plasmon resonance on a BIACORE 2000 apparatus (Biacore, GE Healthcare, Sweden) at the protein core facility in SUNYSB, to determine the affinity of the two drugs for APE1 (or $\text{N}\Delta 40$ APE1). APE1 and its mutants (10 μg) (RU_{max} values were 9000 RU units after immobilization) were immobilized on a CM5 chip by amine coupling (as per the manufacturer's instructions) and binding experiments were performed at 20°C in 10 mM HBS-EP buffer, pH 7.4. Lucanthone (or hycanthone) (20–700 μM) was injected as analyte over the sensor chip in HBS-EP buffer at 10 $\mu\text{l}/\text{min}$. The regeneration was achieved by 10 mM glycine-HCl, pH 3.0 between each analyte (drug) concentration.

Circular Dichroism

APE1 and its mutant proteins (10 mg/ml), 50 μl (500 μg) (14 μM) in APE1 buffer (50 mM HEPES, pH 7.4, 150 mM KCl, 5 mM MgCl_2), were mixed with lucanthone/hycanthone (1 mg/ml), 50 μl (50 μg), 140 μM and incubated at 37°C for 60 min and far UV-CD spectra were recorded at NSLS U11 beam line at BNL. Lucanthone and hycanthone were also scanned as drug controls. The scanning parameters used were a 0.001 cm path length quartz cell, scanning wavelengths from 260 to 170 nm, bandwidth of 0.5 nm, digital integration time of 1 s, time constant of 200 ms, step size of 1 nm, and sensitivity of 200 μV . The data were corrected with blank subtraction from APE1 buffer alone. The secondary structure for APE1 with or without lucanthone or hycanthone was analyzed using CDSSTR program DICHROWEB [38].

MALDI-TOF

100 nM of APE1 protein was treated with 100 μM of lucanthone, hycanthone or CRT at 37°C for 2 h and 24 h and analyzed on sinipinic acid matrix on a Voyager-DE STR (Applied Biosystems) MALDI-TOF instrument at the Proteomics facility at SUNYSB in a linear mode.

Ape1 fragment identification by MALDI-TOF and LC/MS

The full length APE1 and its 25 kDa fragment were digested in gel by trypsin and analyzed by MALDI-TOF and LC/MS. Voyager-DE STR (Applied Biosystems) MALDI-TOF instrument at the Proteomics facility at SUNYSB in a reflector mode was used and the matrix was Alpha-cyano-4-hydroxycinnamic Acid (CHCA).

Docking studies

The screening used the AutoDock suite of programs [39–41]. The screening was driven by a set of scripts described in Mezei *et al* [42]. Models of lucanthone and hycanthone were generated with Marvin Sketch (figure S1) (ChemAxon, Budapest, Hungary), and the structures optimized with the semiempirical AM1 method, as implemented in Gaussian-03 [REF_G] – the script set referred to above includes utilities to create the Gaussian input and the extraction of the optimized coordinates. The terminal amine was protonated, as determined previously and the overall structures were in good agreement with the X-ray structure of hycanthone [43]. The protein structure was obtained from the Protein Data Bank (PDB ID: 2ISI). Assignment of atom types, and partial charges (using Gasteiger –Marsili method) and merging of non-polar hydrogens with their carbons was performed with AutoDockTools

(<http://mgltools.scripps.edu/downloads>). The generation of the energy grids, the preparation of ligand files for docking and the actual docking was driven by a script that keeps a user-defined number of docking jobs running on different processors of our SGI cluster [42].

Dockings were based on a $126 \times 106 \times 126$ grid, with grid spacing of 0.375 Å that targeted the hydrophobic pocket lined by hydrophobic amino acids Trp280, Phe266 and Leu282. The minimization resulting in docked poses was performed using Lamarckian genetic algorithm (LGA) and pseudo-Solis and Wets method. Each LGA job consisted of 200 runs with 270, 000 generations in each run and maximum number of energy evaluations of 2,000,000. After clustering of the docked poses by Autodock the program Dockres (URL: <http://inka.mssm.edu/~mezei/dockres>) sorted cluster representatives of the docked poses and extracted the list and coordinates of the top-scoring ones in complex with the target protein.

Molecular dynamics (MD) simulations

The docking top-scoring poses APE1-lucanthone and APE1-hycanthone were solvated, using VMD [44], in a water box extending 10 Å beyond the edge of the complex in all directions, using the TIP3P water model [45]. The system was neutralized with chloride ions and consisted of a total of ~36,100 atoms. MD calculations were performed with NAMD [46] using the AMBER99SB force field [47]. The ligand parameters were determined with ANTECHAMBER [48] using the General Amber Force Field (gaff) [49]. Partial atomic charges were determined with the AM1-BCC method. The systems were energy minimized with 10,000 steps of conjugate gradient energy minimization, followed by gradual heating from 0 to 310 K in 30 ps, and then maintained at constant temperature and pressure (1.01325 bar). The simulations were carried with periodic box conditions, with a 2 femtosecond time step, a uniform dielectric constant of 1, a 1–4 scaling value of 0.833333, a cutoff of non-bonded forces with a switching function starting at 10 Å and reaching 0 at 12 Å, PME with a tolerance of 10^{-6} , and all bonds involving hydrogens constrained with the SHAKE algorithm. A production run was performed for 30 ns and the trajectories were analyzed with VMD.

EMSA assay

In order to elucidate whether lucanthone and hycanthone could inhibit APE1 by interfering with APE1-DNA interaction through their DNA intercalation ability, we measured the DNA binding capacity of APE1 in the presence of lucanthone and hycanthone by incubating different concentrations of APE1 (10 nM and 25 nM) with 100 μM of lucanthone and/or hycanthone for 30 min and subsequently incubating the mixture with 25 nM of THF-containing substrate at 25°C in binding buffer (50 mM HEPES, pH 7.5, 150 mM NaCl, 0.1 mg/ml BSA, 0.5 mM EDTA and 1 mM DTT) for 30 min. THF stands for tetrahydrofuran that represents a synthetic abasic site. This is commonly inserted into an oligonucleotide substrate for measuring APE1 cleavage activity. 5'-incision of THF by APE1 results in a residue that mimics reduced 5'-deoxyribose phosphate group. Since THF group lacks the 1'-OH group, it blocks β-elimination that is required for mediating any dRP lyase activity. The sequence of the APE1 substrate with THF group is 5'CTGCAGCTGATGCGCFGTGCGGATCCGGTGC-3' as described by Liu *et al* [50].

APE1-DNA complex was then separated from unbound substrate DNA by electrophoresis under native conditions in a

1% agarose-0.1% acrylamide gel at 4°C for 1.5 h as described previously [50–51].

Results

Lucanthone/hycanthone promotes APE1 cleavage

Previously, we created an APE1 overexpressor glioma cell line, the U251 1–5 clone [52], to determine the contribution of APE1 to radio-resistance. Since past studies had shown that lucanthone inhibits DNA and RNA synthesis [53] [54] with or without affecting protein synthesis [53], we determined the effect of lucanthone on APE1 protein expression in the U251 1–5 APE1 overexpressor cell line pre-treated with 10 μg/ml cycloheximide (CHX) (a protein synthesis inhibitor) for 4 h. We found that *de novo* APE1 synthesis was not affected significantly, as seen by the near normal levels of intact APE1 in CHX treated cells (Figure 1). However, lucanthone and hycanthone were found to induce cleavage of APE1 as seen by the formation of a 25 kDa fragment.

To begin to define the mechanism of cleavage, we treated whole cell extracts from the U251 1–5 APE1 overexpressor clone with increasing concentrations of lucanthone (2.5–100 μM) and examined APE1 protein stability in the presence of a protease inhibitor cocktail. We found that lucanthone at 50 and 100 μM caused APE1 cleavage and/or degradation as evidenced by a decrease in the full-length 35.5 kDa fragment and an increase in a ~25 kDa fragment (Figure 2). These data suggested a direct effect of lucanthone on APE1 protein integrity, as effects on gene expression are not relevant in this paradigm. It is highly unlikely that the drug preparation was contaminated with a protease, as the compound was synthesized by organic methods *de novo* and handled to avoid any protease contamination. In addition, we found no evidence of non-specific degradation of other control proteins, such as tubulin and human NTH1 (human Nth was used as a DNA repair enzyme control, since like APE1, human Nth has a disordered N-terminus; data not shown).

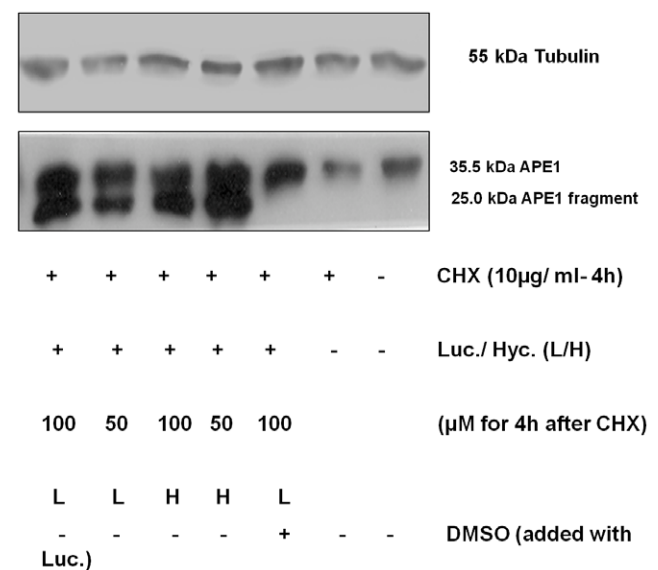


Figure 1. Lucanthone/Hycanthone promotes APE1 cleavage in presence of CHX and this cleavage is inhibited by 1% DMSO. Western blot of total cell extract from APE1-5 overexpressor clone pretreated with 10 μg/ml of cycloheximide for 4 h followed by 25–100 μM lucanthone/hycanthone for 2 h (12.5 mg of total cell protein loaded per lane).

doi:10.1371/journal.pone.0023679.g001

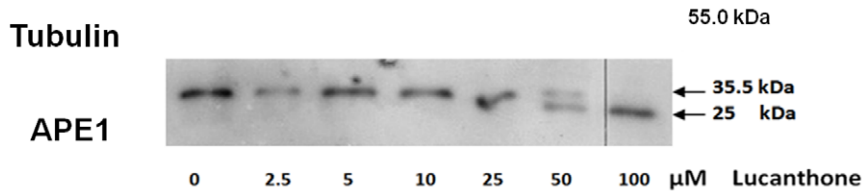


Figure 2. Lucanthone promotes APE1 cleavage in presence of protease inhibitor. Western blot of APE1 over expresser clone 5 pretreated with increasing (2.5–100 μM) concentration of lucanthone in presence of protease inhibitor cocktail for 2 h at 37°C (10 μg of total cell protein loaded per lane). An arrow indicates the corresponding increase in APE1 25 kDa fragment in last two lanes with a decrease in 35.5 kDa APE1 protein. doi:10.1371/journal.pone.0023679.g002

We next determined the effect of lucanthone, as well as CRT, a commercially available APE1 inhibitor modeled to bind at the hydrophobic site of the protein [13], on the stability of APE1 and tubulin in the presence of a protease inhibitor cocktail. As shown in Figure 3, we found that lucanthone caused cleavage of APE1 at 50 μM in U251 1–5 whole cell extracts, whereas for similar cleavage to occur with CRT, we needed to use 200 μM of the inhibitor. The tubulin protein was unaffected by lucanthone, but showed some shift in its migration at 200 μM CRT.

Recombinant full length APE1 is also cleaved by lucanthone

To further delineate the mechanism of lucanthone-induced cleavage, studies were performed with recombinant full length APE1 protein. When the recombinant protein was treated with 10–50 μM lucanthone at 37°C for 2 h, we observed an increase in the formation of the 25 kDa fragment and a corresponding decrease in AP endonuclease activity (Figure 4A and 4B). When we studied the kinetics of inhibition shown by lucanthone, we found that lucanthone appeared most likely to be a non-competitive inhibitor of APE1 (Figure 4B). When human Nth was treated with lucanthone, we did not observe any cleavage (data not shown), indicating specificity for APE1. These data imply that lucanthone directly binds to APE1.

As we observed that lucanthone/hycanthone induced cleavage of APE1, we determined if this cleavage might be due to oxidative damage of the peptide bonds in the protein. We therefore performed an experiment in the presence of the short and long lived radical quenchers: 10 mM (final) tris(hydroxymethyl)aminomethane

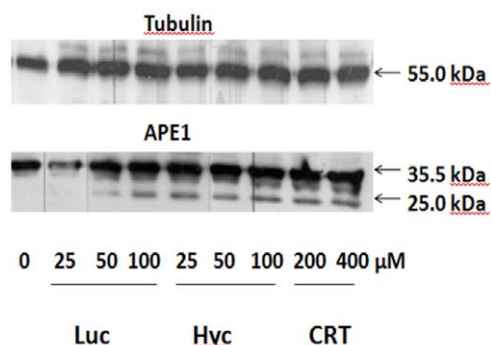


Figure 3. Lucanthone/Hycanthone promote APE1 cleavage at lower concentration than CRT. Western blot of APE1 over expresser clone 5 pretreated with increasing concentration of lucanthone (2.5–100 μM) and CRT0044876 (2.5–200 μM) in presence of protease inhibitor cocktail for 2 h at 37°C (10 μg of total cell protein loaded per lane). The corresponding decrease in 35.5 kDa APE1 protein band and increase in 25-kDa-degradation product is indicated by the arrows. doi:10.1371/journal.pone.0023679.g003

(TRIS), 100 μM ascorbic acid or 100 μM N-acetyl cysteine (for purified APE1 protein) and 1% DMSO (for APE1 protein from overexpressor cell extracts), and found that lucanthone-induced cleavage of APE1 was significantly inhibited (Figure 5 and Figure 6). As lucanthone is made of a strong hydrogen bonding acid, a

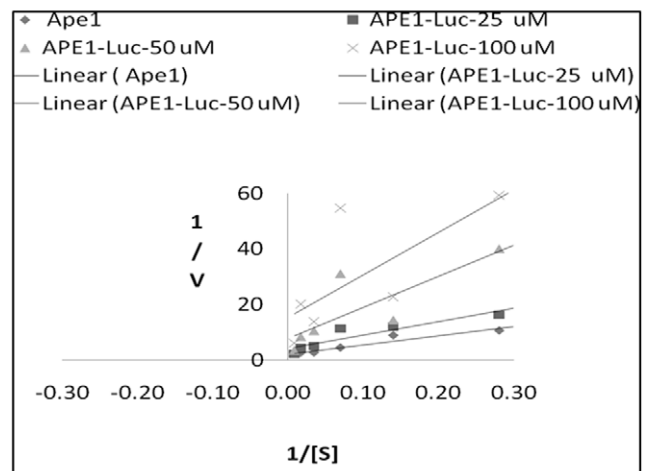
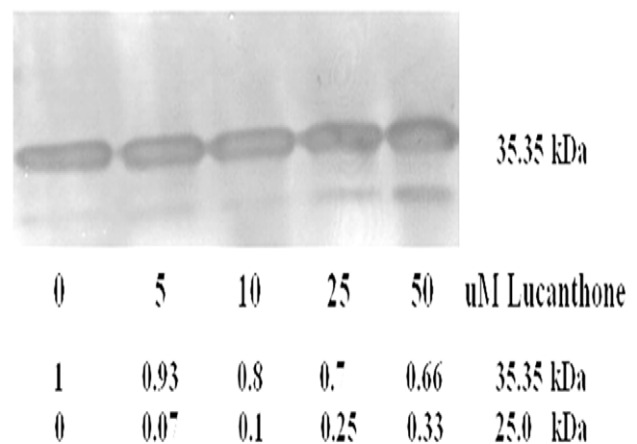


Figure 4. Lucanthone promotes APE1 cleavage *in vitro* by possible non-competitive binding. A. Recombinant APE1 protein (250 ng) treated with 10–50 μM lucanthone at 37°C for 2 h, the numbers in italic font represent fold change in APE1 and its 25 kDa fragment as measured by area analysis using Image J quantification program. B. Lineweaver-Burke plot for endonuclease assay determinations as detailed in Materials and Methods. Units of 1/v were min/fmoles of abasic sites incised and for 1/[S] was inverse of nM of depurinated plasmid DNA. doi:10.1371/journal.pone.0023679.g004

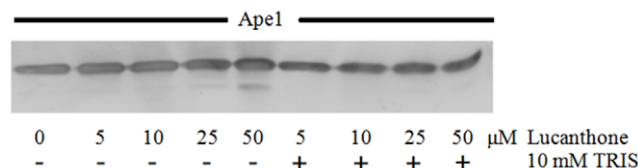


Figure 5. Lucanthone promotes APE1 cleavage in vitro which is inhibited by TRIS. Western blot of recombinant APE1 protein (250 ng) treated with 10–50 μ M lucanthone at 37°C for 2 h in absence and presence of radical quencher, 10 mM Tris-HCl, pH 7.4. doi:10.1371/journal.pone.0023679.g005

secondary amine and two proton bonding bases (the carbonyl and tertiary amine substituent) and is known to possess a strong intramolecular amino carbonyl hydrogen bond [32], which can possibly attack the amide linkage in APE1, this may be one of the ways it can affect APE1 integrity.

APE1 directly interacts with lucanthone and hycanthone

CD spectral studies revealed considerable conformational changes in APE1 in the presence of either lucanthone or hycanthone, indicating a direct physical interaction between the protein and small molecule (Figure 7). In particular, a significant change in the helical portion of the protein was evident, as seen by a decrease in the average helical length per segment (Table 1).

To further characterize the apparent molecular interaction between APE1 and lucanthone/hycanthone, direct binding studies were undertaken using measurements of surface plasmon resonance relative response units (RU) on a BIACORE 2000, which can determine the binding constant, as well as the rates and the stoichiometry of the reaction [48]. In these experiments, a very good binding response was observed between APE1 and hycanthone (Figure 8, top), with weaker binding to lucanthone (Figure 8, bottom). The association phase was weak for lucanthone (see Figure 8, bottom and Table 2), whereas for hycanthone there was a much stronger association, with the k_a and k_d of full length APE1 being about 10-fold higher and 100-fold lower, respectively, for hycanthone. The spike in RU value seen with lucanthone may be due to the initial injection coupled with poor binding, which causes an uneven plateau formation (these seen also figure S2); when higher concentration was used, a clear plateau was seen (figure S2). The negative values seen for lower concentrations of lucanthone are most probably due to very poor interaction of lucanthone with APE1 under BIACORE binding conditions, which when compared to buffer control resulted in no surface plasmon resonance. As the drugs were dissolved in distilled water,

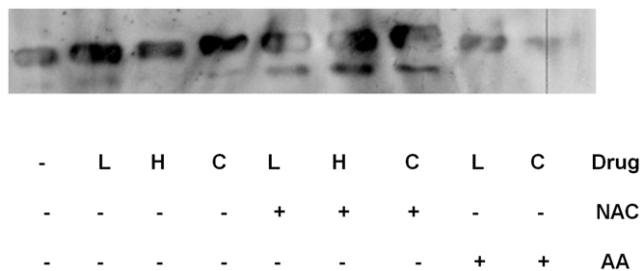


Figure 6. Thioxanthenones and CRT cleavage of APE1 is inhibited by Ascorbic acid but not by N-Acetyl cysteine. Western blot of recombinant APE1 protein (250 ng) treated with 100 μ M of radical quenchers, NAC and Ascorbic acid and 100 μ M of lucanthone (L)/hycanthone (H) or 200 μ M of CRT (C) at 37°C for 2 h. doi:10.1371/journal.pone.0023679.g006

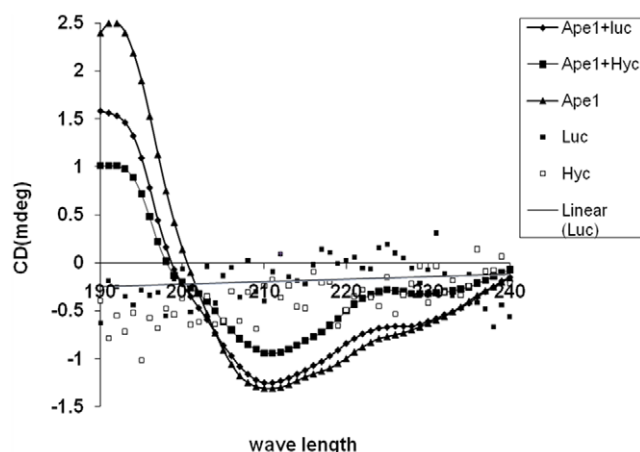


Figure 7. Lucanthone and hycanthone directly alter APE1 conformation. CD spectra of APE1 in presence of lucanthone and hycanthone as described in materials and methods, which was analyzed by Dichroweb program CDSSTR. doi:10.1371/journal.pone.0023679.g007

we did not see any precipitation until 1 mM. The APE1:lucanthone/hycanthone stoichiometry appeared to be close to 1 for hycanthone, but may have been lower for lucanthone. “r” versus Cfree plot was done to determine the differences in affinity of lucanthone and hycanthone and it was clear that hycanthone had much higher binding affinity as compared to lucanthone.

Lucanthone Cleavage site identification with LC/MS

Preliminary data with sequence identification of APE1 protein (sample 1) and its 25 kDa fragment (sample 3) found the cleavage site to be between amino acid (aa) 53–63 resulting in about a 20 kDa fragment as shown in Figure 9. Peptide analysis of aa 64–73 reveals that sample 3 begins at aa 64 and that this peptide is about 100 times lower in concentration in sample 3. Peptide analysis of aa 282–299 reveals that sample 3 ends after aa 299. Peptide aa 53–63 is not present in sample 3. It appears that the degraded protein (sample 3) has peptide present from aa 64 until at least aa 299. Peptide aa 53–63 is not present, suggesting that the cut/degradation is in the vicinity of aa 53–63. The precise N-terminal sequence identification is needed to get the exact cleavage site and studies are under way to determine that site.

Degradation of APE1 by lucanthone and hycanthone

MALDI TOF analysis was undertaken for samples analyzed previously (SDS-PAGE/western blot; see earlier) to determine the nature of the APE1 protein fragments in the presence of lucanthone, hycanthone, or CRT at 37°C for 2 or 24 h. These studies revealed steady degradation of APE1 into smaller fragments (Figure 10) by lucanthone with time; the signal of the parent 35.5 kDa peak was also significantly reduced, consistent with APE1 breakdown. CRT treatment at the same concentration resulted in much less cleavage of APE1, with the 35.5 kDa peak remaining almost intact, particularly at 2 h, and only a couple of smaller fragments of 10, 12 and 17 kDa appearing at 24 h. Hycanthone showed cleavage of APE1 as evidenced mainly by 10, 11 and 17 kDa peaks, without the other smaller fragments seen with lucanthone. By 24 h at 37°C, the full length APE1 peak was almost completely degraded in the lucanthone/hycanthone treated samples, whereas there was still an intact 35.5 kDa peak with CRT (Figure 10). Even though we saw cleavage of recombinant APE1, we did not see the 25 kDa fragment observed

Table 1. Changes in APE1 conformation in presence of lucanthone and hycanthone.

Sample	Helix 1	Helix 2	Av. helix length per segment	Strand 1	Strand 2	Av. strand length per segment	Turns	Unordered
APE1	0.01	0.069	4.512	0.261	0.140	5.791	0.126	0.394
APE1 +Luc	0.00	0.071	4.053	0.262	0.140	5.762	0.125	0.403
APE1 +Hyc	0.00	0.069	4.020	0.267	0.141	5.799	0.124	0.399

Differences in CD conformation in presence of Lucanthone and Hycanthone. Data in Table 1 represent the CD analysis of APE1 in presence of lucanthone and hycanthone (Figure 7) which are shown as changes in α helix, β sheet and unordered conformation of APE1 protein. APE1 protein (5 mg/ml), 50 μ l (250 μ g) in APE1 buffer (50 mM HEPES, 150 mM KCl, 5 mM MgCl₂), was mixed with lucanthone/hycanthone (1 mg/ml), 50 μ l (50 μ g), incubated at 37°C for 60 min and far UV-CD spectra were recorded at NSLS U11 beam line at BNL. These data are representation of three independent repeats.

doi:10.1371/journal.pone.0023679.t001

in the extract studies or recombinant protein experiments described above (Figures 1 and 4). However, as we did see fragments of 10–17 kDa on MALDI, it is possible that the 25 kDa fragment degraded into these smaller fragments during the analysis.

Molecular docking of lucanthone and hycanthone at the hydrophobic site of APE1

To examine possible binding modes of lucanthone and hycanthone with APE1, in silico molecular docking was performed with the AutoDock suite of programs (Figure 11). To account for the flexibility of structural elements and aa side chains, the top-scoring pose of each ligand (based on the energy evaluation of AutoDock and clustering of the poses) was fully solvated and submitted to a 30 ns MD simulation. After an initial equilibration in which the protein side chains and the ligand re-adjusted their positions, the ligands were in a stable conformation for up to the 30 ns simulated, undergoing an average rmsd <2 Å for the second half of the simulation (data not shown). Overall, the docked complexes of APE1-lucanthone and APE1-hycanthone superpose with the MD simulated structures with an r.m.s.d. (root mean square deviation) of 1.8 Å/1.7 Å (Figure 12A and B). Lucanthone binds deep in the hydrophobic pocket (Figure 12A), interacting with the protein mainly via apolar contacts. The phenyl group of lucanthone forms a parallel-displaced pi-stacking interaction to Phe266, while the carbonyl group forms a transient hydrogen bond with Thr268, with an average distance of 3.4 Å between donor and acceptor throughout the simulation. The long flexible side chain of the tertiary amine of lucanthone extended to the DNA binding groove. The hycanthone binding site was shifted towards the DNA binding groove and the unsubstituted ring was buried in the hydrophobic pocket of the protein, in a position to form a parallel pi-stacking interaction with Phe266. The hydroxyl group of hycanthone formed a stable hydrogen bond with His309, while the oxygen atom was stably coordinated with the APE1 bound magnesium cation (Figure 12B). The flexible side chain of hycanthone extended into the solvent and made no protein contacts.

Hydrophobic site mutants do not undergo dramatic conformational changes in the presence of lucanthone

In light of the docking studies above, and since previous APE1 inhibitors (e.g. CRT and L-DOPA) were postulated to interact in a similar manner with the protein [13,55], we determined whether mutating a single hydrophobic site residue, Phe266 to Ala/Cys (F266A or F266C), or mutating two hydrophobic residues, Phe266Ala/Trp280Ala (F266A/W280A), would prevent the lucanthone-induced conformational changes in APE1.

Bovine serum albumin (BSA) was included as a non-specific protein control and the active site APE1 mutant Asp210Arg (D210N) was included as a non-hydrophobic site control, presenting the same binding ability but failing to cleave the DNA. Human NTH1 and *E.coli* endonuclease IV (Nfo) were used as other DNA repair enzyme controls. As shown in Figure 13, lucanthone was able to induce conformational changes in the wild type and D210N active site mutant APE1 proteins, but altered the hydrophobic site mutant protein F266A or F266C to a lesser extent, while inducing almost no conformational change in the double mutant F266A/W280A. Lucanthone also caused little conformational changes on human Nth and *E.coli* Nfo. These data indicate the importance of the hydrophobic site residues F266 and W280 in binding the small molecule inhibitor, and support the binding mechanism proposed by molecular modeling.

Hydrophobic site mutants are not cleaved by lucanthone and show lower inhibition of their endonuclease activity in the presence of lucanthone

As we found that F266A, F266C or F266A/W280A proteins did not undergo a significant conformational change in the presence of lucanthone, we hypothesized that due to impaired binding, lucanthone would show a lesser effect on protein cleavage and endonuclease incision efficiency [34]. As seen in Figure 14A and B, all the hydrophobic site mutants, except W280S, did not undergo cleavage (this W280S mutant also showed conformational change, figure S3), whereas the active site mutant D210N, His309Ser (H309S) and His309Arg (H309N) were degraded. In addition, lucanthone caused a corresponding inhibition of the endonuclease activity of wild type, but no inhibition was detected for the already reduced activity of the single mutants (F266A or W280S), whereas the effect on endonuclease activity of the double hydrophobic mutant's endonuclease activity could not be detected, as this double mutant (F266A/W280A) had very reduced activity as reported earlier [56].

Lucanthone and hycanthone only marginally inhibit the DNA binding capacity of APE1

As lucanthone and hycanthone are well known DNA intercalators, preferentially intercalating at AT rich sites in DNA, we determined whether inhibition of APE1 endonuclease activity was due to compound-DNA interactions, which may block APE1 access to the abasic substrate. The results from a gel mobility shift assay demonstrated that both lucanthone and hycanthone, which were pre-incubated with the protein prior to incubation with the substrate DNA, only marginally inhibited or failed to inhibit APE1 DNA binding capacity as shown in Figure 15.

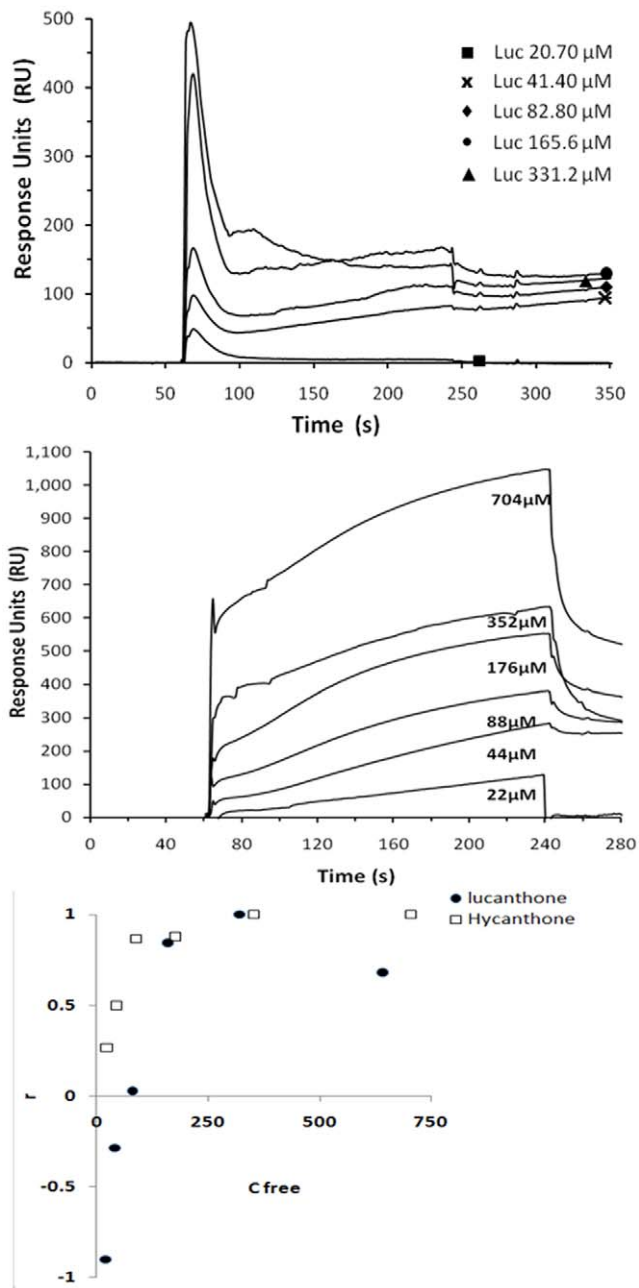


Figure 8. APE1 binds directly with lucanthone and hycanthone with different affinities. APE1 protein (100 μ g) (ligand) was immobilized on carboxymethyl-5 (CM-5) chip by amine coupling according to manufacturer's instructions. Hycanthone (top figure) (analyte) and lucanthone (analyte) (lower figure) (analyte) at different concentrations (as shown as numbers representing μ M values) were tested for binding to APE1 on BAICORE 2000 SPR measurement system available at SUNYSB proteomics core facility. The observed maximum response (RU) was determined by direct curve fitting of the obtained data assuming a 1:1 interaction model. The third sub figure shows plot of r (RU/RU_{max}) versus C_{free} . Binding studies were carried out 3 times and data presented are representative of those 3 separate experiments. doi:10.1371/journal.pone.0023679.g008

Discussion

Our recent studies [10] showed that APE1 plays a significant role in the survival of the glioblastoma cell line U87 as compared to U251. Indeed, we found a direct correlation between the level

Table 2. Kinetics of lucanthone and hycanthone binding to APE1.

Inhibitor	Conc (μ M)	RU_{ligand}	RU_{max}	k_a (1/Ms)	k_d (1/s)	KD (nM)
LUC	20	-82	91	878	7.76×10^{-5}	89
	40	-26				
	80	2.5				
	160	77				
	320	94				
	640	62				
HYC	22	24	90	90	8.9×10^{-7}	10
	44	45				
	88	78				
	176	79				
	352	90				
	704	118				

Hycanthone shows higher binding affinity as compared to Lucanthone. Data in Table 1 show affinity analysis of lucanthone (LUC) and hycanthone (HYC) binding to APE1 immobilized on CM5 chip (Figure 6A and 6B) using BIAsimulation software available at the Biacore facility at SUNYSB. RU = Resonance units are measure of changes in refractive index; k_a = association constant; k_d = dissociation constant and KD = Affinity constant. These data are representation of two independent repeats. doi:10.1371/journal.pone.0023679.t002

of APE1 expression and radio-resistance. In addition to our APE1 overexpressor studies with the radio-sensitive cell line U251, we also showed that suppressing APE1 protein levels with the small molecule inhibitor lucanthone caused radio-sensitization. Lucanthone was chosen as an APE1 inhibitor for several reasons: It is in a Phase I clinical trial for tumor radiotherapy, its side effects are almost negligible, and it can inhibit APE1 endonuclease activity without affecting its redox function. However, as lucanthone has good DNA intercalation ability, we hypothesized that the final outcome of APE1 inhibition might be due to a fine balance between direct and indirect effects. Thus, we sought to elucidate the mechanism of APE1 endonuclease inhibition by lucanthone.

As APE1 has a well-characterized hydrophobic site within its active site, we hypothesized those small hydrophobic molecules like lucanthone may stack in this site through van der Waals interactions and thus alter the active site causing repair endonuclease inhibition. When we treated U251 1–5 glioma cells with increasing concentrations of lucanthone, we observed a concentration-dependent decrease in the normal 35.5 kDa APE1 protein band, along with an increase in a 25 kDa fragment. Since this fragmentation was seen in the presence of protease inhibitors, it is not likely the result of enzyme-mediated proteolysis, but may occur due to a direct effect of lucanthone on the APE1 protein. We reproduced the finding of lucanthone induced APE1 degradation with purified recombinant protein, indicating that the cell machinery was not required for the cleavage event. MALDI TOF analysis of APE1 protein treated with lucanthone or hycanthone revealed a significant degradation of the 35.5 kDa peak and lower molecular weight species, although the 25 kDa fragment could not be found. This observation may suggest that the 25 kDa fragment is further degraded into smaller fragments. Sequencing of the 25 kDa APE1 fragment by MALDI TOF indicated the approximate cleavage site to be between aa 53–63. Our finding that short and long lived free radical quenchers, such as TRIS, ascorbic acid and DMSO, inhibit this degradation implies that protein fragmentation may be facilitated through a

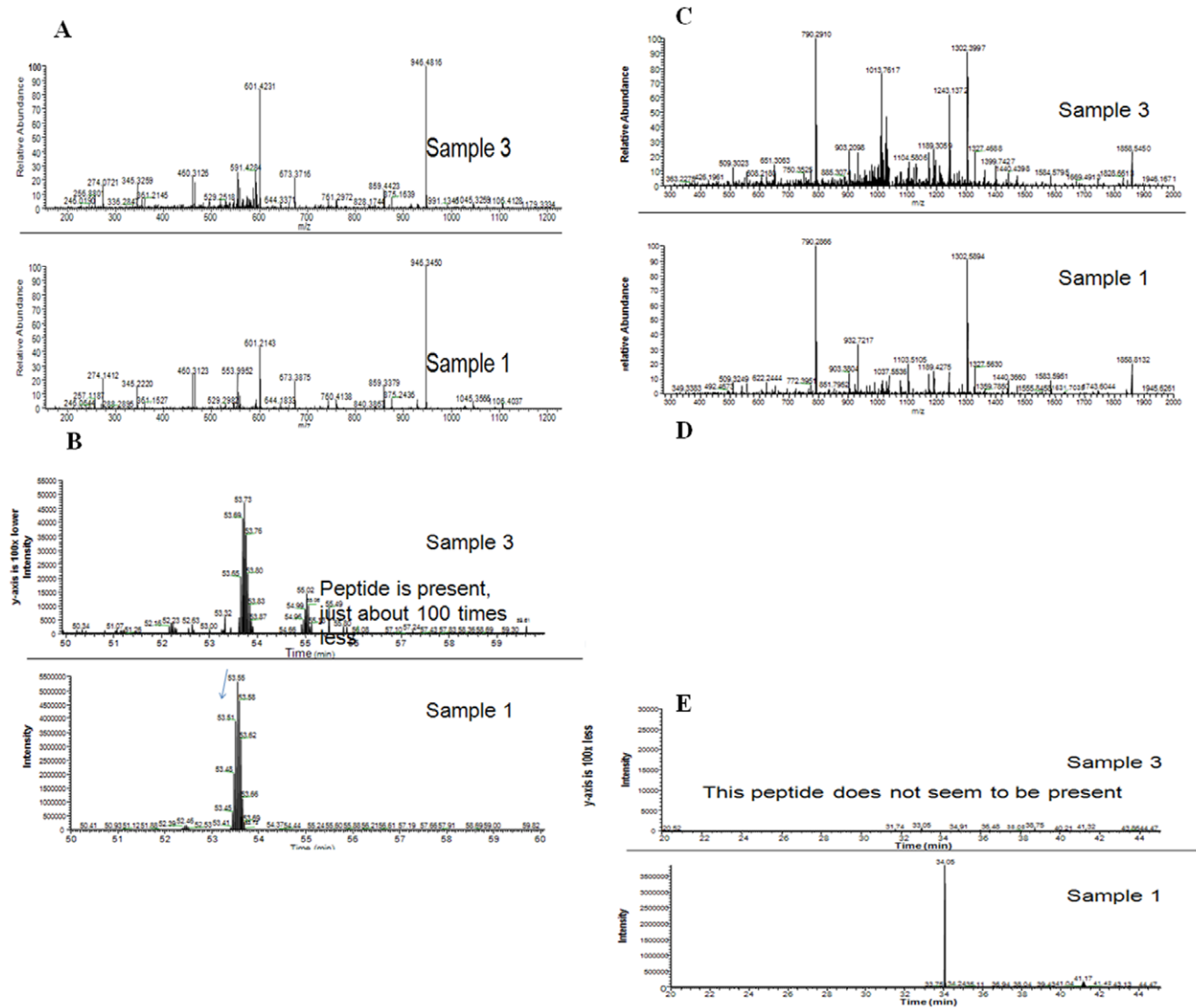


Figure 9. Identification of an approximate lucanthane cleavage site in APE1. LC/MS/MS identification of APE1 fragment after treatment with 100 μ M of lucanthane for 2 h at 37°C. The data were analyzed with Inspect. A). Peptide aa64–73 analysis of 35.5 Kda (Sample 1) and 25 kDa (Sample 3). B). Elution profile of peptide aa64–73 in sample 1 and 3. C). Peptide aa282–299 analysis of 35.5 Kda (Sample 1) and 25 kDa (Sample 3). D). Peptide aa53–63 analysis of 35.5 Kda (Sample 1) and 25 kDa (Sample 3). B). Elution profile of peptide aa53–63 in sample 1 and 3. doi:10.1371/journal.pone.0023679.g009

free radical mediated peptide bond cleavage reaction. The lack of inhibition of this cleavage by N-acetyl cysteine may indicate that a higher concentration of this free radical quencher may be needed or that thioxanthenones are able to render this quencher ineffective.

Our molecular docking, biochemical and biophysical studies, including those using various hydrophobic site and active site mutant APE1 proteins, support our hypothesis that lucanthane docks at the hydrophobic site. Furthermore, another APE1 inhibitor study found that several potent APE1 inhibitors contain two negatively charged ionizable groups separated by a hydrophobic core [57], features characteristic in lucanthane/hycanthane. As recently shown for the phenyl ring of the APE1 inhibitor, 6-hydroxy-DL-DOPA [55], the tri phenyl ring of lucanthane could form a pi stacking interaction with Phe266. Since our binding studies revealed that the K_a for hycanthane is about 8-fold higher than lucanthane, additional interactions between the

former compound and the APE1 active site can be implied. Indeed, molecular docking revealed that in addition to key non-covalent van der Waals interactions seen with lucanthane, the extra hydroxyl groups of hycanthane can hydrogen bond with His309 and coordinate the APE1 bound magnesium cation. Our experimental studies found that lucanthane exhibited a lesser effect on the conformational status of the APE1 single hydrophobic site mutants F266A and F266C, and almost no effect on the double hydrophobic mutant F266A/W280A, consistent with no cleavage or significant effect on the endonuclease activity of these mutants (Figure 12A and B). However, surprisingly, we did see significant cleavage with W280S indicating that replacing the tryptophan residue with a serine did not alter the lucanthane induced cleavage. This is in stark contrast to the dramatic inhibition observed when phenylalanine was replaced by an alanine or cytosine, presumably reflecting lucanthane being able to bind the phenylalanine residue at 266 (as well as leucine at 282).

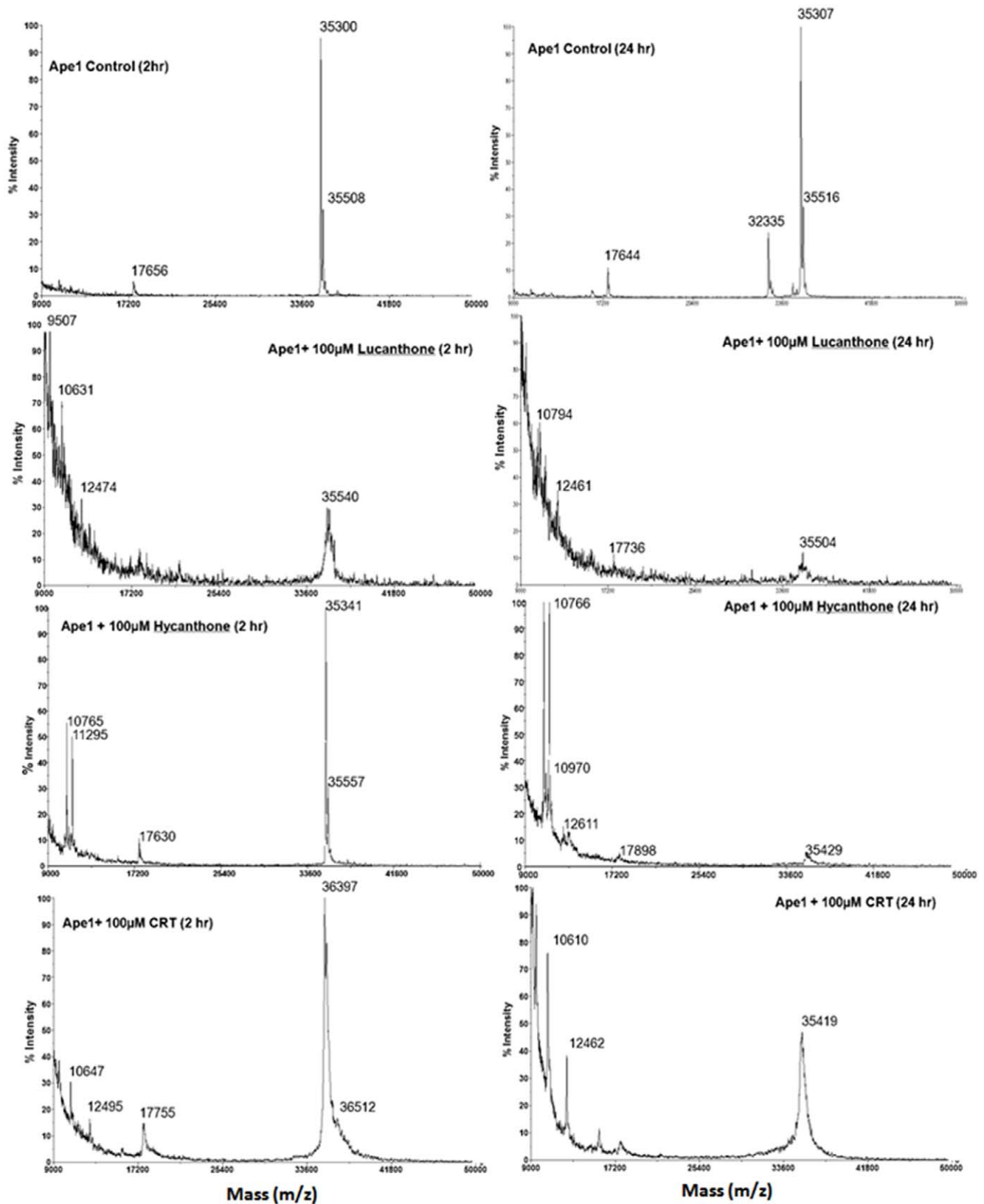


Figure 10. Lucanthone, Hycanthone and CRT cause APE1 degradation. Mass spectroscopic (MALDI-TOF) analysis of APE1 in presence of lucanthone and CRT as described in materials and methods. APE1 (100 μM) was treated with 100 μM lucanthone and CRT for 2 h and 24 h and changes in its mass was determined as described in Materials & Methods. doi:10.1371/journal.pone.0023679.g010

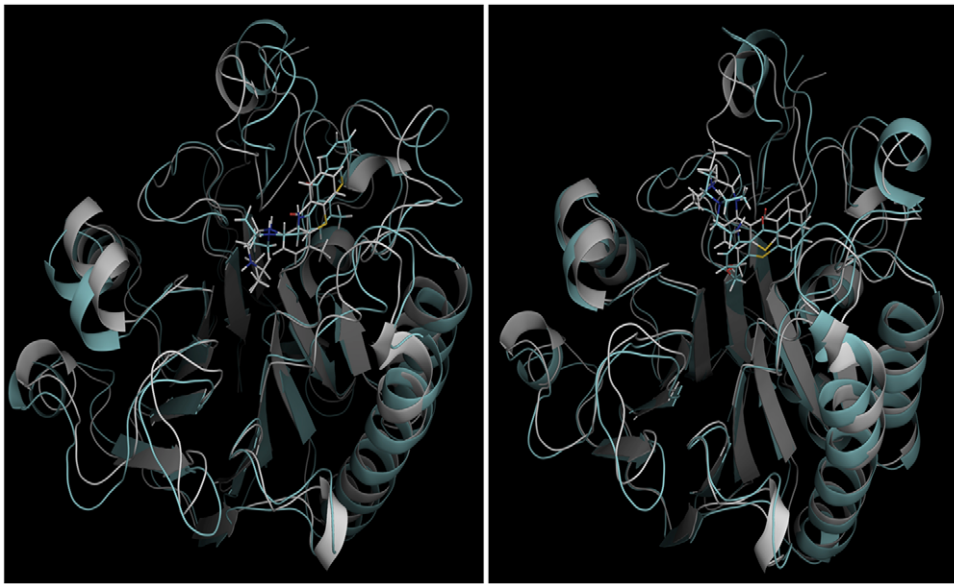


Figure 11. Lucanthonone and hycanthonone docks at hydrophobic site in APE1. A) The lowest energy pose of docked APE1/lucanthonone (gray) superposes with the structure of the complex post 30 ns of MD simulation with an r.m.s.d. of 1.8. Å. B) docked APE1/hycanthonone (gray) superposes with the structure of this complex post 30 ns of molecular dynamics simulation with an r.m.s.d. of 1.7. Å. doi:10.1371/journal.pone.0023679.g011

Apparently F266 is the more critical residue involved in lucanthonone binding.

We used another APE1 specific inhibitor CRT0044876 as a control, as it was modeled to bind to the hydrophobic site [13]. However, the effects of this inhibitor are unclear, as recent data on CRT have shown that its specificity for APE1 is controversial [58–60]. Nonetheless, in our cell system, CRT could inhibit APE1 protein at high concentrations (200 μ M), as opposed to the inhibition we observed by lucanthonone at 50 μ M. The MALDI analysis also revealed clear degradation of APE1 in the presence of

100 μ M lucanthonone by 2 h, whereas at the same concentration, CRT0044876 did not cause degradation of APE1 until 24 h. These studies indicate that lucanthonone and hycanthonone are more potent APE1 inhibitors than CRT0044876.

As lucanthonone and hycanthonone were first used as DNA intercalators with good anti-tumor activity, another aspect of the inhibition of APE1 endonuclease activity likely involves an indirect effect. For instance, like the indirect effect seen for lucanthonone or IA-5 on Topoisomerase II [61], the lucanthonone–DNA intercalation may cause a distortion in DNA, leading to an

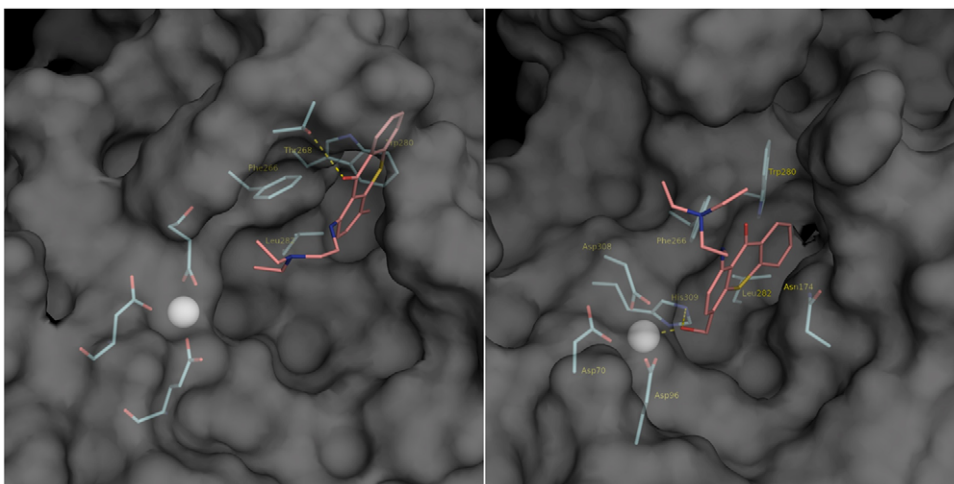


Figure 12. Molecular Dynamics simulation of APE1-bound Lucanthonone and Hycanthonone. A) lucanthonone (magenta sticks) binds in the hydrophobic pocket of Ape1, represented by its solvent accessible surface. Ape1 interacts with lucanthonone mainly via apolar contacts with W280, pi-stacking with F266, and M270. Additionally, a hydrogen bond forms between the carbonyl oxygen and T268. B) Hycanthonone (magenta sticks) binds in the DNA groove/hydrophobic pocket of APE1. In addition to apolar contacts and pi-stacking with F266, it forms a hydrogen bond with His309 and coordinates with the APE1-bound magnesium cation (represented as gray sphere). doi:10.1371/journal.pone.0023679.g012

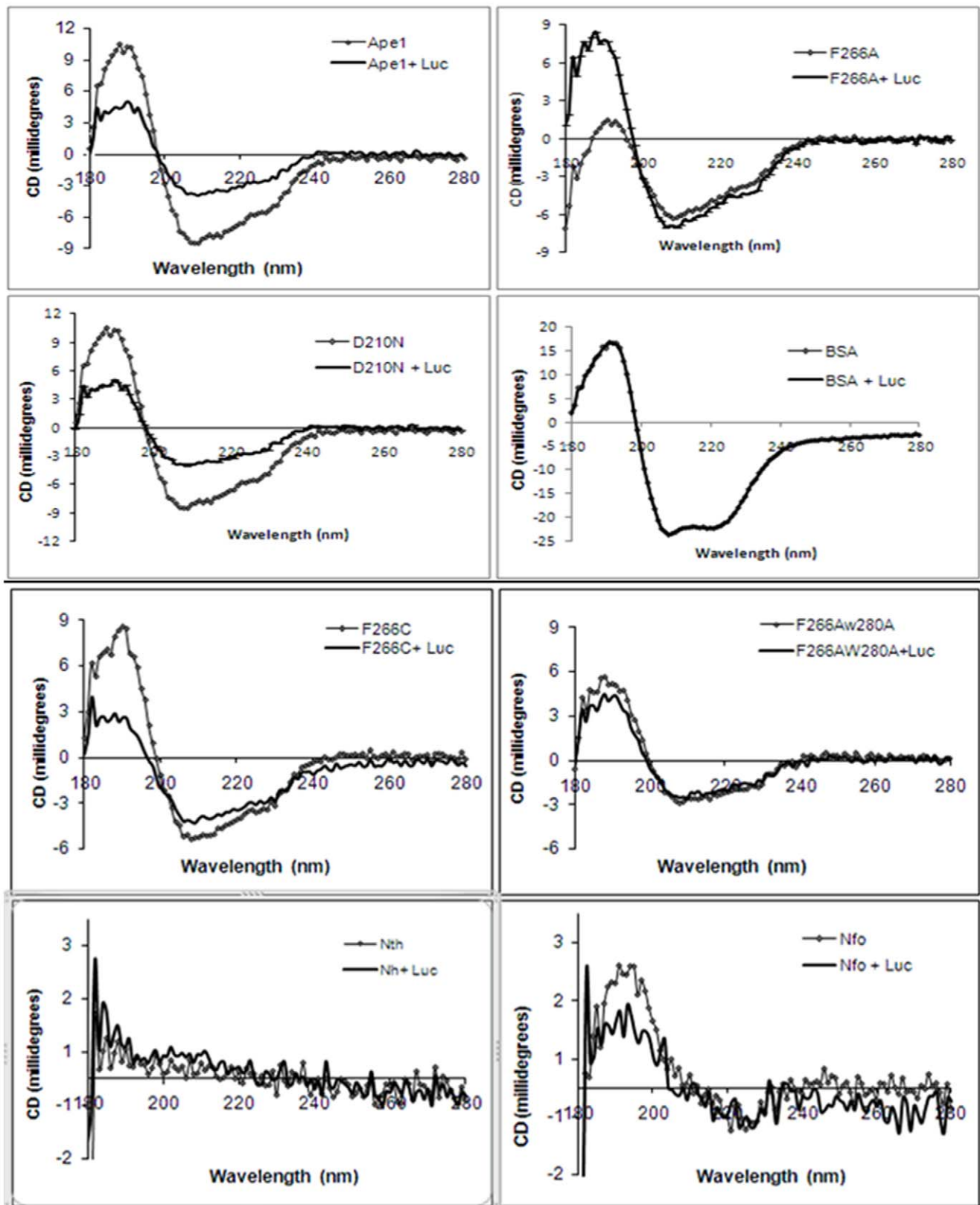


Figure 13. Lucanthone does not alter conformation of double hydrophobic site APE1 mutant, human Nth and bacterial Nfo proteins. CD spectra of APE1 and its mutants in presence of lucanthone. APE1- hydrophobic site mutant proteins F266A/C, F266A/W280A, active site mutant D210N and non-related BSA protein or human Nth or E.coli Nfo(10 mg/ml), 50 μ l (500 μ g) (14 μ M) in APE1 buffer (50 mM HEPES, 150 mM KCl, 5 mM $MgCl_2$), was mixed with lucanthone (1 mg/ml), 50 μ l (50 μ g) (140 μ M), incubated at 37°C for 60 min and far UV-CD spectra with specifications.

doi:10.1371/journal.pone.0023679.g013

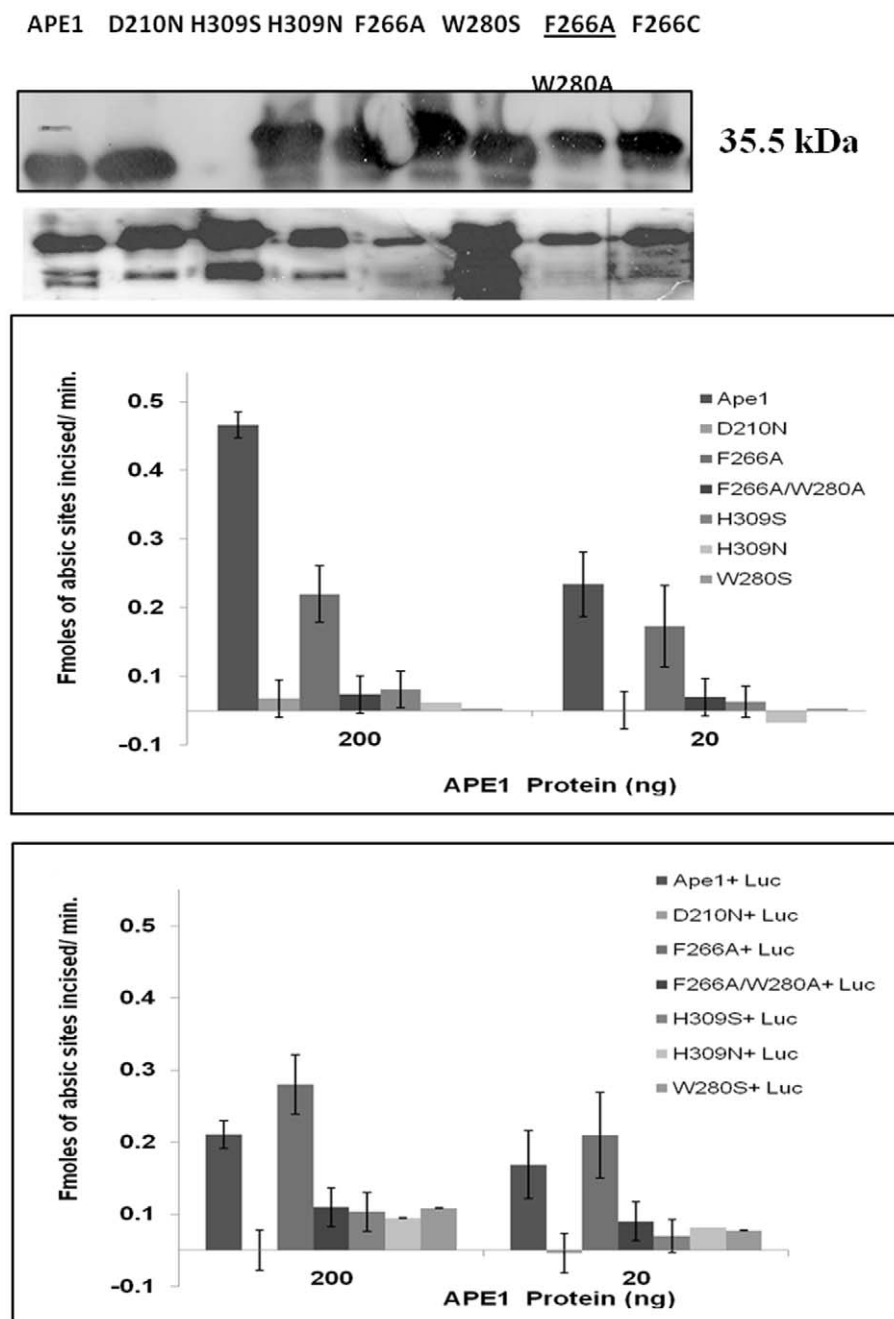


Figure 14. Lucanthone causes cleavage of APE1 with intact hydrophobic site. (A). Western blot of recombinant and mutant APE1 proteins (upper panel) treated with 100 μ M lucanthone (lower panel) at 37°C for 2 h. (B). Endonuclease activity inhibition of wild type and F266A mutant of APE1 in presence of 100 μ M of lucanthone for 2 h at 37°C. doi:10.1371/journal.pone.0023679.g014

impaired recognition of an abasic site by APE1. However, it is important to note that researchers have found no quantitative correlation between the ability of thioxanthenones to bind DNA and their antitumor ability [62], indicating that DNA intercalation is not sufficient for antitumor activity. These studies therefore indicate an important role for other macromolecules like proteins, such as DNA repair enzymes and accessory factors like HMGB1, in the potency of these compounds. Since the DNA binding ability of APE1 was only marginally altered by lucanthone and not by hycanthone, our data indicate that the

effect of lucanthone is more likely due to its direct effect on the enzymology of APE1. Although lucanthone induced cytotoxicity has been attributed more to inhibition of Topo II [63], our present study, along with the past biochemical and cellular effects reported, indicate that APE1 is likely an important biological target. We therefore believe that APE1 may be developed as a biomarker for lucanthone-based treatment efficacy and that these studies provide a molecular framework for the design of more efficacious and clinically safe thioxanthenones.

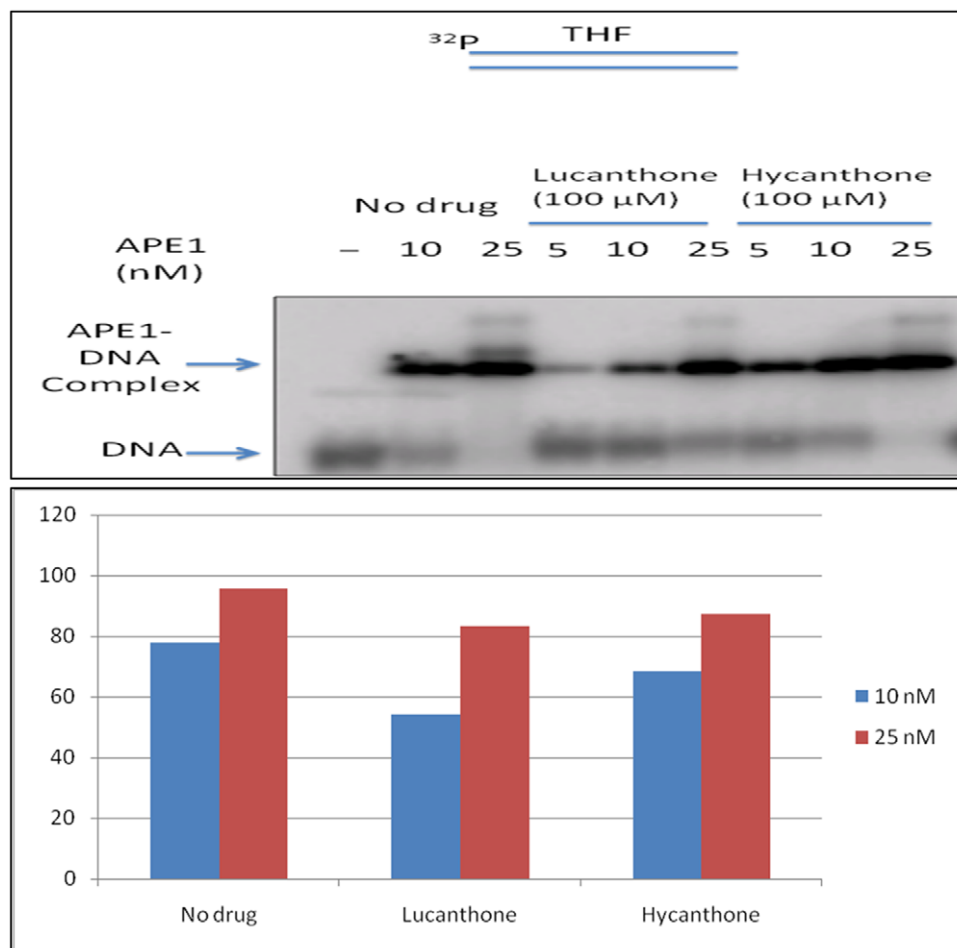


Figure 15. Lucanthone and Hycanthone do not significantly affect the DNA binding capacity of APE1. Gel mobility shift assay for determining the effect of lucanthone and hycanthone on DNA binding capacity of APE1. APE1 at 10 nM and 25 nM was mixed with 100 μM lucanthone or 100 μM hycanthone in the buffer that contained 50 mM HEPES, 150 mM KCl, 0.1 mg/ml BSA, 0.5 mM EDTA and 1 mM DTT. The mixture was incubated at room temperature for 30 min. Subsequently, 10 nM radiolabeled substrate that contained an abasic site was added in the mixture and incubated with the enzyme for additional 30 min to allow binding of APE1 to the substrate. 8 μl binding mixture was subject to electrophoresis at 4°C, 100 V for 1.5 h in a 1% agarose–0.1% acrylamide gel. The gel was then dried on DE81 paper, and APE1-DNA complex was detected by phosphorimager as described previously [52].
doi:10.1371/journal.pone.0023679.g015

Supporting Information

Figure S1 Lucanthone (left) and Hycanthone (right). The Molecular structure was generated with Marvin Sketch.
(TIF)

Figure S2 Lucanthone binding with APE1 reached saturation at higher concentration. APE1 protein (100 μg) (ligand) was immobilized on carboxymethyl-5 (CM-5) chip by amine coupling according to manufacturer's instructions. lucanthone (analyte) with higher concentration (20–1325 μM) was tested for binding to APE1 on BAICORE 2000 SPR measurement system available at SUNYSB proteomics core facility.
(TIF)

Figure S3 CD spectra of APE1 and its mutant W280S in presence of lucanthone. APE1/W280 S (10 mg/ml), 50 μl (500 μg) (14 μM) in APE1 buffer (50 mM HEPES, 150 mM KCl, 5 mM MgCl₂), was mixed with lucanthone (1 mg/ml), 50 μl

(50 μg) (140 μM), incubated at 37°C for 60 min and far UV-CD spectra with specifications taken as described previously.
(TIF)

Acknowledgments

We would like to express thanks to Dr. Betsy Sutherland (posthumus) and Dr. Fritz Henn for their support to MN, Dr. S. Swaminathan for his support to RA, Drs. Bruce Demple, Tahadide Izumi and Sankar Mitra for their expression plasmids and valuable suggestions and Dr. Devendra Naidu for his help with figures of the paper.

BNL is managed by Brookhaven Science Associates, L.L.C. for the U.S. Department of Energy under Contract DE-AC02-98CH10886.

Author Contributions

Conceived and designed the experiments: MN. Performed the experiments: MN RA LC ZS MS YL PC. Analyzed the data: MN LC MM YL. Contributed reagents/materials/analysis tools: LP DMW SHW MJW. Wrote the paper: MN DMW.

References

- Izumi T, Brown B, Naidu CV, Bhakat KK, MacInnes M, et al. (2005) Two essential but distinct functions of the mammalian abasic endonuclease. *Proc Natl Acad Sci U S A* 102(16): 5739–5743.
- Wilson III DM, Barsky D (2001) The major human abasic endonuclease: formation, consequences and repair of abasic lesions in DNA. *Mutation Research/DNA Repair* 485(4): 283–307.
- Xanthoudakis S, Miao GG, Curran T (1994) The redox and DNA-repair activities of ref-1 are encoded by nonoverlapping domains. *Proc Natl Acad Sci U S A* 91: 23–27.
- Chen DS, Herman T, Demple B (1991) Two distinct human DNA diesterases that hydrolyze 3'-blocking deoxyribose fragments from oxidized DNA. *Nucleic Acids Res* 19(21): 5907–5914.
- Fishel M, Vasko MR, Kelley MR (2007) DNA repair in neurons: So if they don't divide what's to repair? *Mutation Research/Fundamental and Molecular Mechanisms of Mutagenesis* 614(1–2): 24–36.
- Bobola MS, Finn LS, Ellenbogen RG, Geyer JR, Berger MS, et al. (2005) Apurinic/apryrimidinic endonuclease activity is associated with response to radiation and chemotherapy in medulloblastoma and primitive neuroectodermal tumors. *Clin Cancer Res* 11(20): 7405–14.
- Silber JR, Bobola MS, Blank A, Schoeler KD, Haroldson PD, et al. (2002) The apurinic/apryrimidinic endonuclease activity of Ape1/Ref-1 contributes to human glioma cell resistance to alkylating agents and is elevated by oxidative stress. *Clin Cancer Res* 8(9): 3008–18.
- Ono Y, Matsumoto K, Furata, Ohmoto T, Akiyama K, et al. (1995) Relationship between expression of a major apurinic/apryrimidinic endonuclease (APEX nuclease) and susceptibility to genotoxic agents in human glioma cell lines. *J Neurooncol* 25(3): 183–192.
- Robertson KA, Bullock KA, Xu Y, Tritt R, Zimmerman E, et al. (2001) Altered expression of Ape1/ref-1 in germ cell tumors and overexpression in NT2 cells confers resistance to bleomycin and radiation. *Cancer Res* 61(5): 2220–5.
- Naidu MD, Mason JM, Pica RV, Fung H, Pena LP (2010) Radiation resistance in glioma cells determined by DNA damage repair activity of Ape1/Ref-1. *J Radiat Res (Tokyo)* 51(4): 393–404.
- Xiang DB, Chen ZT, Wang D, Li MX, Xie JY, et al. (2008) Chimeric adenoviral vector Ad5/F35-mediated APE1 siRNA enhances sensitivity of human colorectal cancer cells to radiotherapy in vitro and in vivo. *Cancer Gene Ther* 15(10): 625–635.
- Luo M, Kelley MR (2004) Inhibition of the human apurinic/apryrimidinic endonuclease (APE1) repair activity and sensitization of breast cancer cells to DNA alkylating agents with lukanthone. *Anticancer Res* 24(4): 2127–34.
- Madhusudan S, Smart F, Shrimpton S, Parsons GL, Gardiner L, et al. (2005) Isolation of a small molecule inhibitor of DNA base excision repair. *Nucleic Acids Res* 33(15): 4711–4724.
- Horton JK, Prasad R, Hou E, Wilson SH (2000) Protection against methylation-induced cytotoxicity by DNA polymerase beta-dependent long patch base excision repair. *J Biol Chem* 275(3): 2211–2218.
- Raffoul JJ, Banerjee S, Singh-Gupta V, Knoll ZE, Fite A, et al. (2007) Down-regulation of apurinic/apryrimidinic endonuclease 1/redox factor-1 expression by soy isoflavones enhances prostate cancer radiotherapy in vitro and in vivo. *Cancer Res* 67(5): 2141–2149.
- Shimizu N, Sugimoto K, Tang J, Nishi T, Sato I, et al. (2000) High-performance affinity beads for identifying drug receptors. *Nat Biotechnol* 18(8): 877–881.
- Kelley MR, Luo M, Reed A, Su D, Delaplane S, et al. (2010) Functional analysis of novel analogs of E3330 that block the redox signaling activity of the multifunctional AP endonuclease/redox signaling enzyme APE1/Ref-1. *Sep 27* [Epub ahead of print].
- Nyland RL, Luo M, Kelley MR, Broch RF (2010) Design and synthesis of novel quinone inhibitors targeted to the redox function of apurinic/apryrimidinic endonuclease 1/redox enhancing factor-1 (Ape1/ref-1). *J Med Chem* 53(3): 1200–1210.
- Nguyen C, Teo JL, Matsuda A, Eguchi M, Chi EY, et al. (2003) Chemogenomic identification of Ref-1/AP-1 as a therapeutic target for asthma. *Proc Natl Acad Sci U S A* 100(3): 1169–1173.
- Jiang Y, Guo C, Fishel M, Wang, Vasko MR, et al. (2009) Role of APE1 in differentiated neuroblastoma SH-SY5Y cells in response to oxidative stress: use of APE1 small molecule inhibitors to delineate APE1 functions. *DNA Repair* 8(11): 1273–1182.
- Yang S, Irani K, Heffern S, Jurnak F, Meyskens FL (2005) Alteration in the expression of Apurinic endonuclease-1/redox factor-1(APE/Ref-1) in human melanoma and identification of the therapeutic potential of resveratrol as an Ape/Ref-1 inhibitor. *Mol Can Therap* 12(4): 1930–1935.
- Bases R, Mendez BA (1997) Topoisomerase inhibition by Lukanthone, an adjuvant in rdiaition therapy. *Int J Radiat Oncol Biol Phys* 37(5): 1133–1137.
- Rosi D, Perruzotti G, Dennis EW, Berberian DA, Freele H, et al. (1965) A New, Active metabolite of 'Miracil D'. *Nature* 208(5014): 1005–1006.
- Berberian DA, Freele H, Rosi D, Dennis EW, Archer S (1967) A Comparison of Oral and Parenteral Activity of Hycanthone and Lukanthone in Experimental Infections with Schistosoma Mansonii. *Am J Trop Med Hyg* 16(4): 487–491.
- Cioli D, Pica-Mattocchia L, Archer S (1995) Antischistosomal drugs: Past, present...and future? *Pharmac Ther* 68(1): 35–85.
- Russell WL (1975) Results of tests for possible transmitted genetic effects of hycanthone in mammals. *J Toxicol Environ Health* 1: 301–304.
- Bulay O, Urman H, Path K, Clayton DB, Shubik P (1979) Carcinogenic potential of hycanthone in mice and hamsters. *Int J Cancer* 23: 97–104.
- Turner S, Bases R, Pearlman A, Nobler M, Kabakow B (1975) The adjuvant effect of Lukanthone(Miracil D) in Clinical Radiation Therapy. *Radiology* 114: 729–731.
- Del Rowe JD, Bello J, Mitnick R, Sood B, Filippi C, et al. (1999) Accelerated regression of brain metastases in patients receiving whole brain radiation and the topoisomerase II inhibitor, lukanthone. *Int J Radiat Oncol Biol Phys* 43(1): 89–93.
- Mendez F, Goldman J, Dand Bases RBE (2002) Abasic sites in DNA of HeLa cells induced by lukanthone. *Cancer Invest* 20(7–8): 983–91.
- Bailly C, Waring MJ (1993) Preferential Intercalation at AT sequences in DNA by Lukanthone, Hycanthone and Indazole Analogs. A Footprinting Study. *Biochemistry* 32: 5985–5993.
- Zilversmit R (1971) Thioxanthones. II. Studies on the hydrogen-bonding capacity of lukanthone. *Mol Pharmacol* 7(6): 674–682.
- Agarwal R, Eshwaramoorthy S, Kumaran D, Dunn JJ, Swaminathan S (2004) Cloning, high level expression, purification, and crystallization of the full length Clostridium botulinum neurotoxin type E light chain. *Protein Expr Purif* 34(1): 95–102.
- Erzberger JP, Barsky D, Schärer OD, Colvin ME, Wilson III DM (1998) Elements in abasic site recognition by the major human and Escherichia coli apurinic/apryrimidinic endonucleases. *Nucleic Acids Res* 26(11): 2771–2778.
- Bobola MS, Blank A, Beger MS, Stevens BA, Silber JR (2001) Apurinic/apryrimidinic endonuclease activity is elevated in human adult gliomas. *Clin Cancer Res* 7(11): 3510–8.
- Futcher AB, Morgan AR (1979) A novel assay for endonucleases acting at apurinic sites and its use in measuring AP endonuclease activity in repair-deficient mutants of Saccharomyces cerevisiae. *Can J Biochem* 57(6): 932–7.
- Sutherland JC, Sutherland BM, Emrick A, Monteleeone DC, Riebero EA, et al. (1991) Quantitative electronic imaging of gel fluorescence with CCD cameras: applications in molecular biology. *Biotechniques* 10(4): 492–7.
- Whitmore L, Wallace BM (2004) DICHROWEB: an online server for protein secondary structure analyses from circular dichroism spectroscopic data. *Nucleic Acids Research* 32(web serve issue): W 668–W 673.
- Morris GM, Goodsell DS, Halliday RS, Huey R, Hart WE, et al. (1998) Automated docking using a Lamarckian genetic algorithm and an empirical binding free energy function. *Computational Chemistry* 19(14): 1639–1642.
- Goodsell DS, Morris GM, Olson AJ (1996) Automated Docking of Flexible Ligands: Applications of AutoDock. *Journal of Molecular Recognition* 9(1): 1–5.
- Huey R, Morris GM, Olson AJ, Goodsell DS (2007) A semi-empirical free energy force field with charge-based desolvation. *J Comp Chem* 28: 1145–1152.
- Mezei M, Zhou MM (2010) Dockres: a computer program that analyzes the output of virtual screening of small molecules. *Source Code for Biology and Medicine* 5: 2.
- Hardgrove Jnr GL, Einstein JR, Wei CH (1983) Structure of p-(p-nitroanilino)-phenyl isothiocyanate, C13H9N3O2S. *Acta Cryst C39*: 616–620.
- Umphrey W, Dalke A, Schulten K (1996) VMD - Visual Molecular Dynamics. *J Mol Graph* 14: 33–38.
- Jorgensen WL, Chandrasekhar J, Madhura JD, Impey RW, Klein ML (1983) Comparison of simple potential functions for simulating liquid water. *J Chem Phys* 79: 926–935.
- Phillips JC, Braun R, Wang W, Gumbart J, Tajkhorshid E, et al. (2005) Scalable molecular dynamics with NAMD. *J Comp Chem* 26: 1781–1802.
- Hornak V, Abel R, Okur A, Stockbine B, Roitberg A, et al. (2006) Comparison of multiple Amber force fields and development of improved protein backbone parameters. *Proteins* 65(3): 712–725.
- Wang J, Wang W, Kollman PA, Case DA (2006) Automatic atom type and bond type perception in molecular mechanical calculations. *J Mol Graph Mod* 25: 247–260.
- Wang J, Wolf RM, Caldwell JW, Kollman PA, Case DA (2004) Development and testing of a general AMBER force field. *J Comp Chem* 25: 1157–1174.
- Liu Y, Prasad R, Beard WA, Kedar PS, Hou ES, et al. (2007) Coordination of Steps in Single-nucleotide Base Excision Repair Mediated by Apurinic/ Apyrimidinic Endonuclease 1 and DNA Polymerase β. *J Biol Chem*, 2007 282(18): 13532–13541.
- Liu Y, Beard WA, Shock PS, Prasad R, Hou ES, et al. (2005) DNA polymerase beta and flap endonuclease 1 enzymatic specificities sustain DNA synthesis for long patch base excision repair. *J Biol Chem* 280(5): 3665–3774.
- Kingma PS, Corbett AH, Burcham PC, Marnett IJ, Osheroff N (1995) Abasic sites stimulate double-stranded DNA cleavage mediated by topoisomerase II. DNA lesions as endogenous topoisomerase II poisons. *J Biol Chem* 270(7): 21441–21444.
- Bases R, Mendez F (1969) Reversible inhibition of Ribosomal RNA Synthesis in HeLa cells by Lukanthone(Miracil D) with continued synthesis of DNA -like RNA. *J Cell Physiol* 74: 283–294.
- Epifanova OI, Makarova GF, Abuladze MK (1975) A comparative study of the effects of lukanthone 9Miracil D) and Actinomycin D on the Chinese Hamster cells grown in cultures. *J Cell Physiol* 86(2): 261–268.
- Simeonov A, Kulkarni A, Dorjsuren D, Jadhav A, Shen M, et al. (2009) Identification and Characterization of Inhibitors of Human Apurinic/apryrimidinic Endonuclease APE1. *PLoS ONE* 4(6): 1–13.

56. Hadi M, Ginalski K, Nguyen LH, Wilson III DM (2002) Determinants in Nuclease specificity of Ape1 and Ape2, Human Homologues of Escherichia Coli Exonuclease III. *J Biol Chem* 277(3): 853–866.
57. Zawahir Z, Dayam R, Deng J, Pereira C, Neamati N (2009) Pharmacophore Guided Discovery of Small-Molecule Human Apurinic/Apyrimidinic Endonuclease 1 Inhibitors. *J Med Chem* 52(1): 22–32.
58. Fishel ML, Kelley MR (2007) The DNA base excision repair protein Ape1/Ref-1 as a therapeutic and chemopreventive target. *Molecular Aspects of Medicine* 28(3–4): 375–395.
59. Guikema JEJ, Liehan AK, Tsuchimoto D, Nakabeppu Y, Strauss PR, et al. (2007) APE1- and APE2-dependent DNA breaks in immunoglobulin class switch recombination. *J Exp Med* Vol. 204(12): 3017–3026.
60. Koll TT, Feis SS, Wright MH, Taniola MM, Richardson MM, et al. (2008) HSP90 inhibitor, DMAG, synergizes with radiation of lung cancer cells by interfering with base excision and ATM-mediated DNA repair. *Mol Can Therap* 7(7): 1985–1992.
61. Dassoneville L, Bailly C (1999) Stimulation of topoisomerase II-mediated DNA cleavage by an indazole analogue of lucanthone. *Biochem Pharmacol* 58(3): 1307–1312.
62. Archer S, Miller KJ, Rej R, Periana C, Fricker L (1982) Ring-Hydroxylated Analogues of Lucanthone as Antitumor Agents. *J Med Chem* 25(3): 220–227.
63. Kelley MR, Fishel ML (2008) DNA Repair Proteins as Molecular Targets for Cancer Therapeutics. *Anticancer Agents Med Chem* 8(4): 417–425.